Kidney International, Vol. 61 (2002), pp. 125–132

Laser microdissection and gene expression analysis on formaldehyde-fixed archival tissue

Clemens D. Cohen, Hermann-Josef Gröne, Elisabeth F. Gröne, Peter J. Nelson, Detlef Schlöndorff, and Matthias Kretzler

Medizinische Poliklinik, Ludwig-Maximilians-University of Munich, Munich, and German Cancer Research Center, Department of Cellular and Molecular Pathology, Heidelberg, Germany

Laser microdissection and gene expression analysis on formaldehyde-fixed archival tissue.

Background. Analysis of renal biopsies is currently based on histological recognition of typical structural patterns and immunohistological detection of protein expression alterations. Both can be performed using formaldehyde as the tissue fixative. As a consequence of recent advances in molecular medicine, mRNA expression analysis may offer an attractive option to obtain functionally relevant information. However, quantification of mRNA expression in human renal biopsies thus far has not been possible in formaldehyde-fixed tissue.

Methods. The present study evaluated a recently reported mRNA extraction protocol. Using this approach gene expression analysis could be performed on formaldehyde-fixed archival renal tissues by laser microbeam microdissection, laser pressure catapulting and real time reverse transcription-polymerase chain reaction.

Results. For an initial feasibility study, the expression of two chemokines (IP-10 and RANTES) in renal transplant rejection was examined. Induction of protein expression in allografts undergoing rejection was demonstrated for both chemokines by immunohistochemistry. The mRNA expression alterations in the defined renal compartments of glomeruli, vessels and tubulointerstitium were quantified using laser microdissection from formaldehyde-fixed, paraffin-embedded or frozen tissue sections. A pronounced increase of mRNA expression compared to controls was demonstrated for IP-10 as well as RANTES with both tissue-processing protocols.

Conclusions. Using formaldehyde as the tissue fixative, information on the disease process can now be obtained by histological, immunohistochemical and gene expression techniques. In the future this may allow the study of activated molecular programs in routine renal biopsies as well as archival tissue samples.

Renal biopsy evaluation is currently based upon three approaches: histological evaluation by light microscopy, demonstration of specific proteins by immunofluorescence and analysis of ultrastructure by electron microscopy [1–3]. The frequently descriptive disease classification based on complex morphological patterns represents a major limitation of the current diagnostic process. Quantification of specific parameters should improve the diagnostic and prognostic value of the invasive biopsy procedure. In this regard, quantitative techniques to study the expression of specific mRNA species on formaldehyde-fixed, paraffin-embedded tissue samples represents a promising approach and in addition would allow analysis of archival tissue. Only a few studies have been able to analyze mRNA from formaldehyde-fixed, paraffin-embedded material [4–7]. All these reports could only determine qualitative changes in gene expression, as crosslinking of proteins to the mRNA by tissue fixatives and the minute quantity of templates in microdissected samples prevented reproducible quantification.

Specht and co-workers recently reported a protocol for the isolation of mRNA from formaldehyde-fixed, paraffin-embedded tumor tissue via the digestion of protein-RNA crosslinks by extended proteinase K incubation [8]. In combination with laser microbeam microdissection and real-time reverse transcription-polymerase chain reaction (RT-PCR) tumor-specific gene expression profiles were obtained.

Laser microdissection of circumscribed nephron segments in cryosections has been demonstrated to be an important tool in renal gene expression analysis with the complex architecture of the kidney [9–11]. It offers the unique opportunity to correlate structural information with gene expression programs on the same tissue sample. The clonal expansion of cells in tumor tissue, as studied by Specht et al [8], results in a predominant cell type with a homogenous gene expression profile. The aim of our study was the transfer of this innovative technology to the mixed cell populations found in microdissected renal tissue compartments.

For this feasibility study, the expression of the two chemokines IP-10 (interferon-γ–inducible protein 10) and

Key words: Real-time reverse transcription-polymerase chain reaction, chemokine, renal allograft rejection, formalin, IP-10, RANTES, kidney rejection.

Received for publication April 9, 2001
and in revised form August 1, 2001
Accepted for publication August 27, 2001

RANTES (regulated upon activation, normal T cell expressed and secreted) was studied in renal allografts undergoing rejection. Immunohistology demonstrated increased expression of both chemokines in renal allografts as compared to control kidney tissue. To evaluate the analysis of mRNA expression in formaldehyde-fixed material, specimens derived from human kidneys surgically removed for severe transplant rejection or renal carcinoma were either formaldehyde-fixed and paraffin-embedded or snap frozen. After approximately one year of storage, the material was laser microdissected in tubulointerstitial, vascular and glomerular compartments and analyzed for expression of IP-10 and RANTES mRNA by real-time RT-PCR. To verify that this technique could be applied for routine biopsies, archival biopsy cores of transplant rejection or histologically normal kidneys also were analyzed. Comparable mRNA expression profiles were obtained for IP-10 and RANTES in all kidneys undergoing rejection independently of the fixation and storage technique.

METHODS

Tissue samples

Tissue sections derived from allograft-nephrectomy specimens removed for renal allograft failure with signs of severe acute and chronic rejection were studied (N = 3; patients aged 14 to 53 years; 2 female and 1 male). Unaffected regions from tumor-nephrectomies served as control tissues (N = 2, patients aged 68 and 54 years; 1 female and 1 male). Material was processed as follows: One part of each specimen was fixed with phosphate buffered saline (PBS)-buffered 4% formaldehyde, paraffin-embedded and stored at room temperature. A second sample was snap frozen in liquid nitrogen and stored at −80°C.

Second, biopsies taken from renal transplants with histologically severe graft rejection (BANFF >IIB [12]) were chosen for analysis (N = 4; aged 50 to 66 years; 2 females and 2 males). Four renal biopsies (patients aged 19 to 23 years; 1 female and 3 males) that were found to show regular renal parenchyma as defined by light microscopy, immunohistology and electron microscopy served as controls. All biopsies had been processed for routine light microscopy and immunohistochemical analysis, that is, immediate fixation in 4% PBS-buffered formaldehyde for 24 hours was followed by paraffin-embedding and storage at room temperature.

Immunohistochemistry by the ABC method

To prepare for immunochemistry using the avidin biotinylated enzyme complex (ABC) method, mouse monoclonal antibodies against IP-10 (10 μg/mL) were obtained from R&D Systems (Wiesbaden, Germany) and against RANTES (10 μg/mL) from Vector Laboratories (Burlingame, CA, USA). Following blockade of endogenous peroxidase activity by incubating the section in 3% H_2O_2 at 22°C for 10 minutes, nonspecific binding sites were saturated with 4% skim milk in PBS, pH 7.6 at 22°C for 20 minutes. The primary antibody was added to the sections for 18 hours at 4°C. Then avidin, followed by biotin (Avidin/Biotin blocking kit; Vector Laboratories), was added to block endogenous biotin, biotin receptor or avidin binding. This was followed by an anti-mouse biotinylated secondary antibody (PharMingen, Heidelberg, Germany) diluted 1:250 in 1% bovine serum albumin (BSA)/PBS at 22°C for one hour. A horseradish-strepavidin-peroxidase complex (Vector Laboratories; SA 5004 diluted 1:200) was incubated at 22°C for one hour. 3-Amino-9-ethylcarbazole or 3,3′-diaminobenzidine substrate kits (SK-4200 or SK-4100 respectively; Vector Laboratories) were used for specific staining. Counter staining was performed with hematoxylin at 22°C for four minutes.

Control experiments for the immunohistochemical demonstrations entailed immunohistology with nonimmune mouse IgG and absence of primary antibody.

Mounting and staining of slides for laser microdissection

A 1.35 μm polyethylene layer was mounted with cyanacrylate glue (UHU, Buehl, Germany) to glass object slides and coated with 0.1% poly-L-lysine (Sigma, Taufkirchen, Germany). Formaldehyde-fixed, paraffin-embedded tissue samples were cut in nominally 5 μm sections on a microtome using disposable blades. Sections were flattened for at least two hours at 40°C. Deparaffinization was performed by two changes of 100% xylene for ten minutes, followed by rehydration in 100, 96, 70% ethanol for five minutes each. Sections were stained after a short rinse in H_2O by hemalaun for 10 seconds, followed by short rinses in H_2O, 70 and 100% ethanol. Sections were air-dried for two minutes.

Cryosections 5 μm thick were prepared on a cryostat in RNase-free conditions and immediately stored at −80°C. Staining was performed by the above protocol.

Laser microdissection

The microdissection apparatus (PALM Laser MicroBeam System; P.A.L.M, Wolfratshausen, Germany) offered a 337 nm pulsed nitrogen laser coupled to an inverted microscope via an illumination path. Under direct visual control, selected tissue compartments (renal arteries, glomeruli, and cortical tubulointerstitium) were isolated from the surrounding tissue by the focused nitrogen laser beam (see later in this article in Fig. 4). For harvesting of the samples, the energy of the laser was increased and the microdissected area catapulted by a single laser shot [7]. The detached tissue samples were then collected in a microfuge cap coated with the respective lysis buffer and mounted above the object slide. The efficiency of

this procedure was verified by visualizing the harvested samples under a second microscope. The cap containing the sample was placed on a microfuge tube filled with 200-μL lysis buffer and transferred to liquid nitrogen. From each biopsy core a total of 20 to 50 glomerular areas from a series of five consecutive sections or corresponding areas of tubulointerstitial and vascular structures were harvested. From all patients and settings two series of sections were processed in parallel and the mean from both analyses was used for further quantification.

Isolation of total RNA

Microdissected specimens from the formaldehyde-fixed tissue samples were harvested in 200 μL lysis buffer [8] containing 2% sodium dodecyl sulfate (SDS), 10 mmol/L Tris-HCl (pH 8.0), 0.1 mmol/L ethylenediaminetetraacetic acid (EDTA; pH 8.0), and 500 μg/mL proteinase K (Sigma). Samples were incubated at 60°C for 16 hours. Control RNA (1 μg total RNA) handled in parallel showed no loss of mRNA during incubation, determined by real-time RT-PCR for glyceraldehyde-3-phosphate dehydrogenase (GAPDH). Tissue microdissected from frozen sections was harvested in guanidine thiocyanate lysis buffer containing beta-mercapto-ethanol. Extraction of total RNA was performed for both tissue preparations by the addition of 200 μL phenol chloroform, precipitation for five minutes at 4°C, and centrifugation for 10 minutes at 16,000 × g. 200 μL isopropyl ethanol, 40 μL sodium acetate (3 mol/L, pH 4.0) and 0.5 μL glycogen (20 mg/mL) were then added to the aqueous phase prior to a one hour precipitation at −20°C. The total RNA was then washed once in 70% ethanol, air-dried and diluted in 10 μL diethyl pyrocarbonate (DEPC)-treated H_2O.

Reverse transcription

Reverse transcription was performed for 60 minutes at 42°C in a volume of 20 μL using a modified Moloney-murine leukemia virus (MMLV) reverse transcriptase (Superscript and respective buffer; Life Technologies, Karlsruhe, Germany). This was performed in the presence of 1 mmol/L dNTPs (Amersham Pharmacia, Freiburg, Germany), 40 U RNase inhibitor (RNasin; Promega, Mannheim, Germany), 2 μL dithiothreitol (DTT; Life Technologies), 2 μL random hexamers (Roche, Mannheim, Germany), and 7 μL of the above RNA solution.

Real-time quantitative RT-PCR

Real-time RT-PCR was performed on a TaqMan ABI 7700 Sequence Detection System (Applied Biosystems, Weiterstadt, Germany) using heat-activated TaqDNA polymerase (Amplitaq Gold, Applied Biosystems). After an initial hold of two minutes at 50°C and 10 minutes at 95°C the samples were cycled 40 times at 95°C for 15 seconds and 60°C for 60 seconds. The cDNA content of each sample was compared with another sample following the ΔΔCt technique [13, 14]. This procedure uses the formula $A_0/B_0 = (1+E)^{(Ct,B-Ct,A)}$, where A_0 is the initial copy number of sample A; B_0, initial copy number of sample B; E, efficiency of amplification; Ct,A, threshold cycle of sample A; and Ct,B, threshold cycle of sample B. The amplification efficiency was defined as 1 as all analyses were performed during the same runs including control dilution series. Similar amplification efficiencies for targets and housekeeping genes were demonstrated by analyzing serial cDNA dilutions showing an absolute value of the slope of log input cDNA amount versus ΔCT (Ct housekeeping gene − Ct target) of <0.1.

Sequences with following gene bank accession numbers served for the design of the pre-developed Taq Man assay reagents (PDAR) or primers and probe (WT-1), purchased from Applied Biosystems: NM001565 (human IP-10), AF043341 (human RANTES), and M33197 (human GAPDH), X51630 (human Wilms tumor antigen (WT-1): sense primer 5′-AAATGGACAGAAGGGCA GAGC-3′, antisense primer 5′-GGATGGGCGTTGTG TGGT-3′, fluorescence labeled probe (FAM) 5′-ACC ACAGCACAGGGTACGAGAGCGA-3′). All these assay reagents do not amplify genomic DNA. This was verified using genomic human DNA samples. Controls consisting of ddH_2O were negative in all runs.

Statistics

All values are mean ± SEM. Correlation was determined by z-test analysis.

RESULTS

Light microscopy and immunohistochemistry

Floride and chronic rejection signs were demonstrated in all allograft tissues analyzed in this study. This included mononuclear cell infiltrate, glomerulitis, tubular damage and vascular subendothelial cell recruitment. Immunohistochemical determination of IP-10 and RANTES showed a high expression level for both chemokines in all investigated renal compartments, including glomeruli, arteries and tubulointerstitium (Figs. 1 and 2).

Microdissection and mRNA expression

Tissue processing for laser microdissection allowed histological identification of the different nephron segments in both formaldehyde-fixed material and cryo-sections. Formaldehyde-fixation, as expected, showed superior resolution and maintenance of structural characteristics (Fig. 3). Tissue compartments could be delineated with the laser and completely harvested for gene expression analysis (Fig. 4).

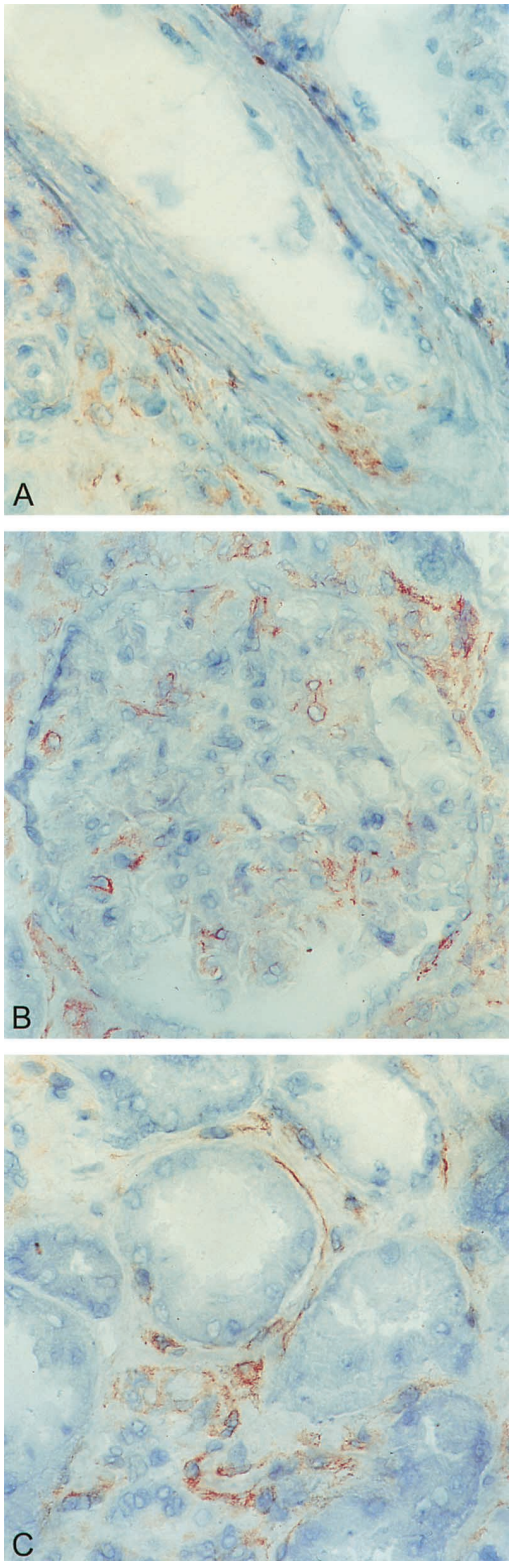

Fig. 1. Interferon-γ–inducible protein 10 (IP-10) positive cells in allograft nephrectomy with acute and chronic rejection phenomena. (*A*) Interlobular artery with IP-10 positive cells subendothelially and in the adventitia (×400). (*B*) Glomerulus with allograft glomerulitis and many IP-10 positive cells in capillary lumina and mesangium (×400). (*C*) Tubules in outer stripe of outer medulla with partly typical partly flattened epithelia of transversely cut tubules which are surrounded by several IP-10 positive mononuclear cells; one IP-10 positive lymphoid cell has infiltrated a tubule (×400). A through C, ABC method for staining.

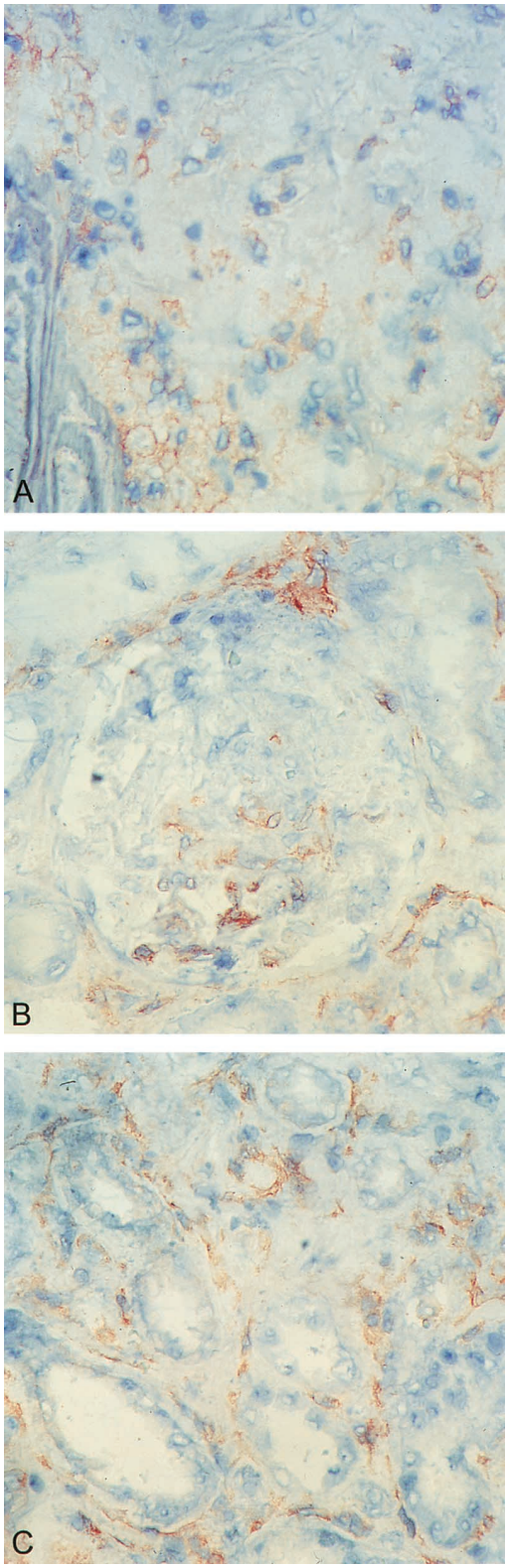

Fig. 2. RANTES-positive cells in allograft nephropathy with chronic vascular rejection, glomerulosclerosis and chronic tubulointerstitial damage. (*A*) Part of the subintimal space of an arcuate artery with foam cells that are labeled at cell periphery and with small-labeled lymphocytes can be seen; vascular lumen is beyond the upper right corner, and lamina elastica interna is at the lower left quadrant of the photograph (×600). (*B*) Glomerulus with segmental sclerosis and RANTES-positive cells in capillary lumina and mesangial areas can be seen in the lower part (×400). (*C*) Chronically damaged tubules with broad basement membranes are surrounded by RANTES-positive mononuclear cells (×400). A through C used the ABC method for staining.

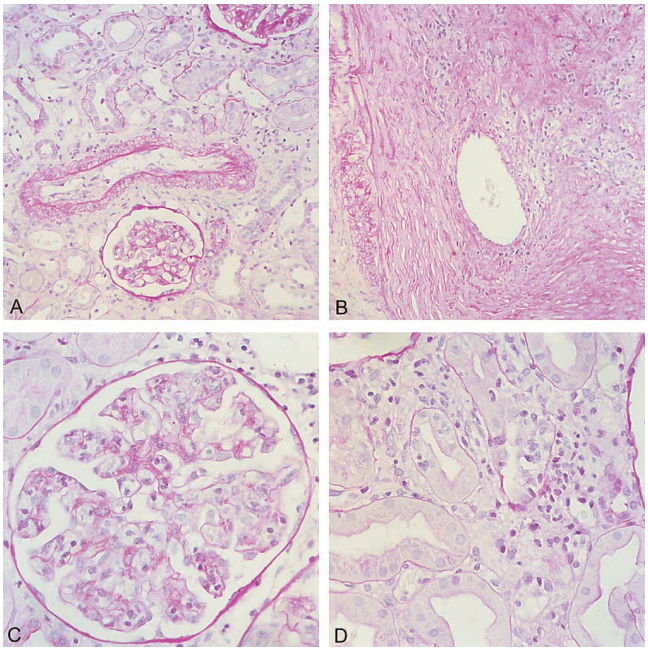

Fig. 3. Light microscopy of vascular, glomerular and tubulointerstitial lesions in renal transplant tissue taken for laser-guided microdissection. (*A*) Intralobular artery with florid vascular rejection. Mononuclear cells can be seen beneath endothelial cells (×200). (*B*) Arcuate artery with chronic rejection. The arterial lumen is severely narrowed. Many foam cells can be seen in the subendothelial space with a pronounced increase in matrix (×200). (*C*) Transplant glomerulitis with mononuclear cells sticking to the edematous activated endothelial cells (×400). (*D*) Florid tubulointerstitial rejection with mononuclear cells in the interstitium and with tubulitis with focal destruction of tubular basement membrane (×400). Panels A through D, PAS staining.

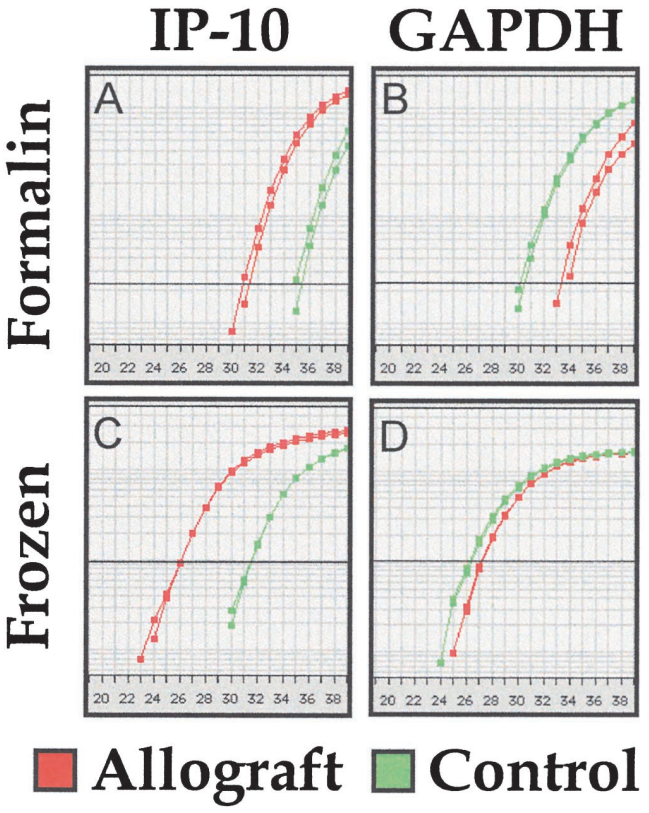

Fig. 5. Real-time RT-PCR for IP-10 and GAPDH. Original amplification data are shown for glomerular samples from transplant (red) and control (green) tissue. Amplification data for IP-10 are shown for formaldehyde-fixed (*A*) and frozen (*C*) sections. (*B* and *D*) Data are for the respective housekeeper GAPDH from the same material. The threshold cycle (Ct, x-axis), measured as the fluorescence intensity above the background (log ΔRn, y-axis) for IP-10, is consistently lower in transplant tissue. This demonstrates a higher IP-10 expression in allografts compared to control material (for GAPDH normalization and further details, see **Methods** section; formalin is formaldehyde).

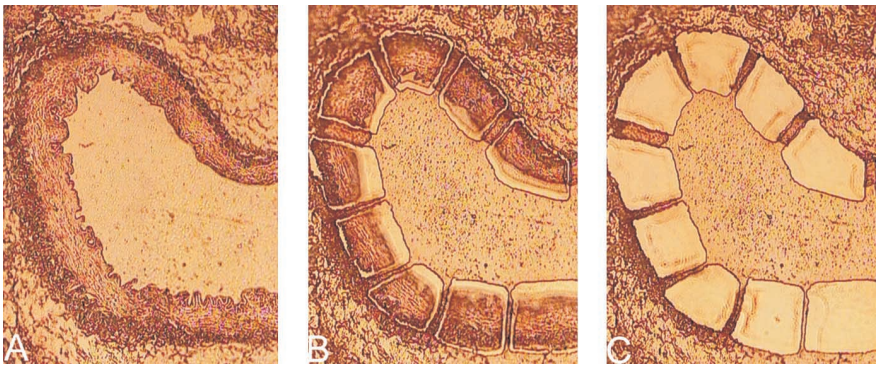

Fig. 4. Laser microdissection of definite organ structures. An interlobular renal artery (*A*) from a formaldehyde-fixed, paraffin-embedded control kidney (unaffected part of a tumor nephrectomy) was laser microdissected in areas adequate for laser pressure catapulting (*B*). After catapulting of the dissected specimen complete harvesting of the tissue is demonstrated (*C*).

Expression levels of the mRNA species were compared between tissue compartments from renal allografts and control material. Parallel processing of the same tissue allowed comparison of formaldehyde-fixation and cryo-preservation. Formaldehyde-fixed biopsies were used to examine the performance of the protocol on material processed under standard conditions for routine diagnostics.

The yield of mRNA recovered from formaldehyde-fixed material was 5.8 ± 1.0-fold (mean ± SEM) lower

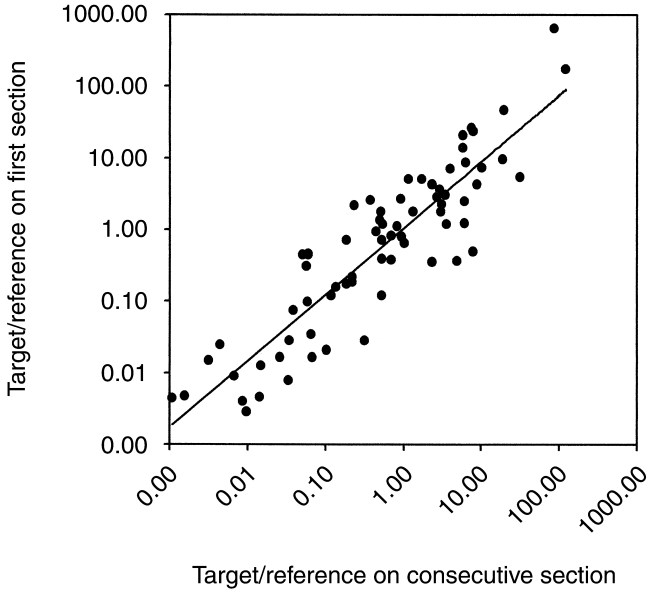

Fig. 6. Correlation between experiments from consecutive sections. Different structural compartments (glomeruli, vessels, tubulointerstitium) were microdissected from consecutive formaldehyde-fixed sections and the expression of IP-10 and RANTES (targets) to the housekeeper GAPDH (reference) determined ($N = 71$). The significant correlation between first and consecutive section indicates a high reproducibility of the quantification (R^2=0.81, $P < 0.01$).

as compared to cryotissue (determined by Ct values for GAPDH, $N = 80$ for each, $P < 0.01$). However, the signal intensity remained well inside the linear range of the assay using as little as the equivalent of four microdissected glomerular cross-sections per reaction (Fig. 5). To study the sensitivity of the technique, WT-1 was analyzed in glomerular, vascular and tubulointerstitial samples ($N = 3$ each). WT-1 was chosen as a low abundant, essentially podocyte-specific transcription factor. As expected, only glomerular samples gave a positive signal for WT-1 (Ct values 29 to 31), all other samples remained negative up to 45 cycles. This demonstrates both the accuracy of the microdissection and the feasibility to study even low abundant mRNA species.

To demonstrate the reproducibility of the microdissection and gene expression analysis, the ratio of IP-10 and RANTES to the housekeeper GAPDH was determined on formaldehyde-fixed, paraffin-embedded samples on serial sections. The gene expression profiles obtained showed a stringent correlation (Fig. 6; $N = 71$, $R^2 = 0.81$, $P < 0.01$), indicating reproducibility of the protocol.

Tissue samples microdissected from cryo-sections, formaldehyde-fixed material, and routine formaldehyde-fixed biopsies showed comparable mRNA expression for IP-10 and RANTES (summarized in Fig. 7).

In tubulointerstitial samples from frozen sections, the mRNA expression of IP-10 was 68 ± 35-fold higher during transplant rejection (mean ± SEM, $N = 3$) as compared to control specimens ($N = 2$). In formaldehyde-fixed nephrectomies a 64 ± 33-fold, and in formaldehyde-fixed routine biopsies a 41 ± 30-fold IP-10 expression above control levels was seen ($N = 4$ for each). Microdissected arteries (1 to 3 vessels per patient) showed a higher expression for IP-10 in rejected organs than in controls (cryo-sectioned nephrectomy, 75 ± 61; formaldehyde-fixed nephrectomy, 228 ± 89; formaldehyde-fixed biopsy, 82 ± 15). In microdissected glomeruli IP-10 mRNA showed an increase of one to two orders of magnitude above control levels (cryo-sectioned nephrectomy, 17 ± 14; formaldehyde-fixed nephrectomy, 123 ± 119; formaldehyde-fixed biopsy, 339 ± 213; Fig. 7A).

A similar magnitude of expression was seen for RANTES during transplant rejection (in the tubulointerstitium: cryo-sectioned nephrectomy, 79 ± 39; formaldehyde-fixed nephrectomy, 126 ± 58; formaldehyde-fixed biopsy, 11 ± 8; in vessels: cryosectioned nephrectomy, 2496 ± 2241; formaldehyde-fixed nephrectomy, 11 ± 6; formaldehyde-fixed biopsy, 197 ± 179; in glomeruli: cryosectioned nephrectomy, 151 ± 114; formaldehyde-fixed nephrectomy, 38 ± 4; formaldehyde-fixed biopsy, 98 ± 60; Fig. 7B).

DISCUSSION

Our study describes a method for quantitative gene expression analysis on laser microdissected, formaldehyde-fixed, and paraffin-embedded renal tissue. This procedure should enable analysis of specific genes on routine diagnostic material and retrospectively on archival tissue samples, material not previously amenable to this type of analysis.

Laser microbeam microdissection has proven to be an elegant tool for the analysis of gene expression of circumscribed organ structures [8, 13]. This is especially important in a heterogeneous organ like the kidney [9–11]. Prior studies using formaldehyde-fixed tissue were only able to demonstrate the absence or presence of specific mRNA templates [4–7]. Goldsworthy et al comprehensively tested different fixation protocols for gene expression analysis by real-time RT-PCR and found a decrease in the yield of cDNA by cross-linking fixatives like formaldehyde as compared to precipitive fixatives, such as ethanol [15]. The authors also demonstrated an increased mRNA yield in frozen sections compared to paraffin-embedded tissue. Therefore, frozen material was used as the sole source for mRNA expression in renal tissue with all inherent problems concerning mRNA stability. Specht and co-workers recently addressed the critical steps required for quantitative gene expression analysis on archival formaldehyde-fixed tissue samples [8]. They found that extensive digestion with proteinase K could degrade the proteins covalently cross-linked to the RNA

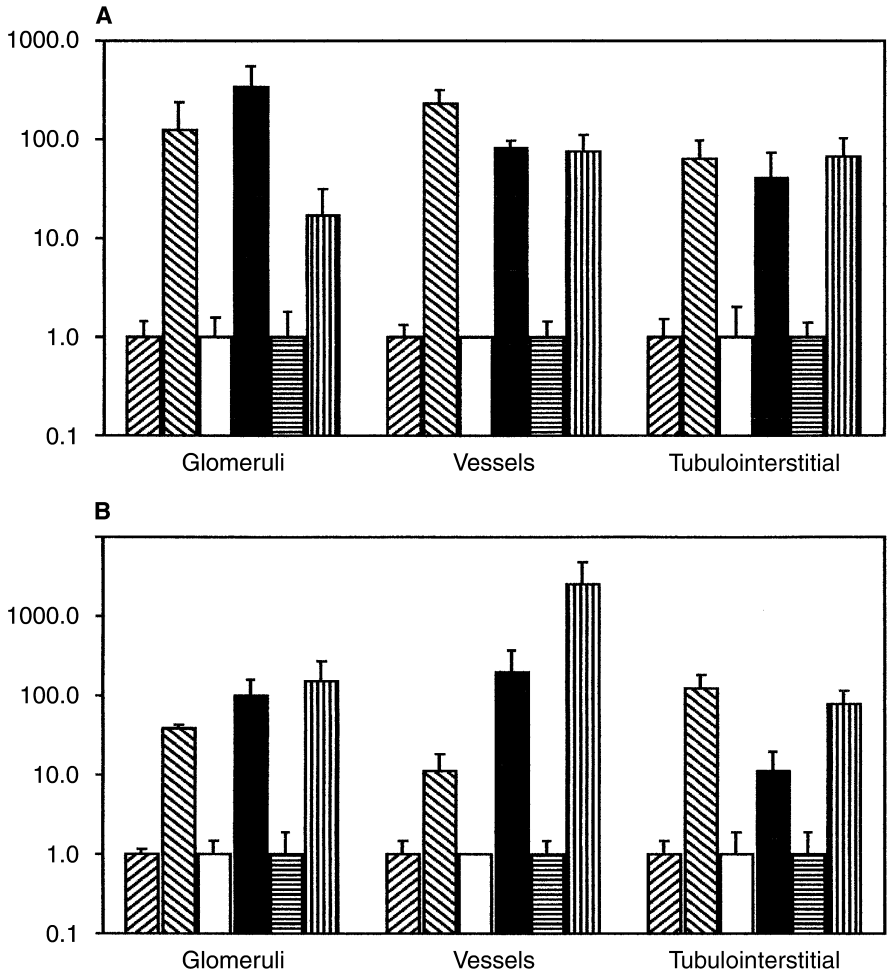

Fig. 7. Summary of IP-10 (*A*) and RANTES (*B*) mRNA expression in allograft rejection and control. Bar graphs represent the mRNA expression of IP-10 and RANTES for each renal compartment in allograft rejection, normalized to control tissue. For all fixation protocols a pronounced increase in the IP-10 and RANTES expression was determined: Tissue from nephrectomies for severe allograft rejection ($N = 3$) or renal cancer (unaffected pole as control, $N = 2$) were either snap frozen or formaldehyde-fixed and paraffin-embedded. Further, routine renal biopsies of allograft rejection or biopsies without significant histopathological alteration ($N = 4$ each) were processed to study the feasibility for routine archival biopsies. Data are shown as mean ± SEM. Symbols are: (▨) formalin control; (▧) formalin TX; (□) formalin con biopsy; (■) formalin TX biopsy; (▤) cryo-control; (▥) cryo-TX.

by the fixation protocol. This reaction was found to be performed best at relatively high temperatures (60°C). Importantly, the authors found that the amplification products had to be as small as possible in order to reduce the inhibition of the RT-PCR by protein-RNA cross-linking events. Real-time RT-PCR is ideally suited for this application, as it combines highly accurate and specific template quantification with the use of small amplicons [16, 17].

In contrast to tumor tissue, inflamed renal tissue represents a heterogeneous cell population, where the normal tissue composition is altered, but not replaced, by infiltrating immune-responsive cells. In this study the applicability of the new protocol was demonstrated for routine renal biopsies. Furthermore, the minute tissue samples allowed the no-contact method of laser pressure catapulting obliterating mechanical cell collection.

Two limitations of the technique became apparent during the study. First, a considerable range of expression is observed, represented by the standard error for each group analyzed. This variation is probably a consequence of the focal nature of inflammatory processes. To exclude that this variation is due to technical variance, chemokine mRNA expression determined on consecutive sections from the same tissue sample were compared. The stringent correlation obtained demonstrated the reproducibility of the microdissection, RNA isolation and quantitative RT-PCR.

The second limitation refers to the amount of RNA available for expression analysis. Formaldehyde-fixed tissue equivalent of four glomerular cross sections were sufficient to allow quantification of one cDNA, limiting the reported protocol for the analysis of a small number of defined molecules. However, the analysis of low abundant mRNA species as WT-1 demonstrates that this new protocol may even allow the examination of target mRNAs of limited expression and distribution. Unfortunately, quality control of the RNA by 28S/18S ratio is not possible as the low amount of mRNA (in the range of picograms) is below the detection limit even of microfluidic systems [18]. But the need for small amplicon sizes for the RT-PCR [4, 8] is consistent with both protein-RNA-interaction and limited degradation. These

limitations of the technique indicate that alternative strategies are needed for broad screening purposes [18].

The present study investigated the expression of two proinflammatory chemokines implicated in renal allograft rejection: IP-10 and RANTES [19]. In previous studies a prominent IP-10 mRNA expression was demonstrated in renal, cardiac and skin allograft rejection [19–21]. Hancock et al showed that the receptor for IP-10, CXCR3, is required for acute cardiac allograft rejection [22]. In the present study IP-10 expression reflected the infiltration seen in all renal compartments. IP-10 positive cells showed vascular subendothelial accumulation and appeared to be involved in glomerulitis and tubular damage. The RANTES mRNA and protein expression confirmed the expression profile described in the rejection of rat [23] and human [24] renal allografts.

Gene expression analysis on formaldehyde-fixed, paraffin-embedded archival tissue samples by laser microbeam microdissection and real time RT-PCR may develop as an important tool to study the mRNA expression changes in renal diseases. It also is a highly attractive option for routine diagnostic application, as it allows histological, immunohistological and gene expression studies using a formaldehyde-fixation protocol established in clinical routine. As a consequence, the tremendous archival tissue resources of pathology institutes are available for retrospective and prospective studies of disease-specific gene expression in humans.

ACKNOWLEDGMENTS

This work was supported by the German Human Genome Project 01KW9922/2, DFG 1492/6-1 and Else Kröner-Fresenius Foundation to M.K. and Deutsche Forschungsgemeinschaft SFB 405/D10 to H.J.G. We thank K. Specht for the kind provision of the RNA isolation protocol and helpful discussion, and C. Schmidt, M. Bonrouhi and K. Frach for excellent technical assistance.

Reprint requests to Dr. Matthias Kretzler, Medizinische Poliklinik, Ludwig-Maximilians-Universität München, Schillerstrasse 42, D-80336, Munich, Germany.
E-mail: kretzler@medpoli.med.uni-muenchen.de

REFERENCES

1. Madaio MP: Renal biopsy. *Kidney Int* 38:529–543, 1990
2. Chandraker A: Diagnostic techniques in the work-up of renal allograft dysfunction-an update. *Curr Opin Nephrol Hypertens* 8: 723–728, 1999
3. Haas M: A reevaluation of routine electron microscopy in the examination of native renal biopsies. *J Am Soc Nephrol* 8:70–76, 1997
4. Heiske A, Anheier B, Pilaski J, *et al*: Polymerase chain reaction detection of Puumala virus RNA in formaldehyde-fixed biopsy material. *Kidney Int* 55:2062–2069, 1999
5. Fink L, Kinfe T, Stein MM, *et al*: Immunostaining and laser-assisted cell picking for mRNA analysis. *Lab Invest* 80:327–333, 2000
6. Kasai T, Shimajiri S, Hashimoto H: Detection of SYT-SSX fusion transcripts in both epithelial and spindle cell areas of biphasic synovial sarcoma using laser microbeam microdissection. *Mol Pathol* 53:107–110, 2000
7. Schutze K, Lahr G: Identification of expressed genes by laser-mediated manipulation of single cells. *Nat Biotechnol* 16:737–742, 1998
8. Specht K, Richter T, Müller U, *et al*: Quantitative gene expression analysis in microdissected archival formaldehyde-fixed and paraffin-embedded tumor tissue. *Am J Pathol* 158:419–429, 2001
9. Kohda Y, Murakami H, Moe OW, Star RA: Analysis of segmental renal gene expression by laser microbeam microdissection. *Kidney Int* 57:321–331, 2000
10. Murakami H, Liotta L, Star RA: IF-LCM: Laser microbeam microdissection of immunofluorescently defined cells for mRNA analysis. *Kidney Int* 58:1346–1353, 2000
11. Grone HJ, Cohen CD, Schmidt C, *et al*: Spatial and temporally restricted expression of adhesion and proliferation-associated chemokines and chemokine receptors in the developing human metanephric kidney. *J Am Soc Nephrol* (in press)
12. Racusen LC, Solez K, Colvin RB, *et al*: The Banff 97 working classification of renal allograft pathology. *Kidney Int* 55:713–723, 1999
13. Fink L, Seeger W, Ermert L, *et al*: Real-time quantitative RT-PCR after laser-assisted cell picking. *Nat Med* 4:1329–1333, 1998
14. Anders HJ, Vielhauer V, Cohen CD, *et al*: Chemokine and chemokine receptor expression during initiation and resolution of immune complex glomerulonephritis. *J Am Soc Nephrol* 12:919–931, 2001
15. Goldsworthy SM, Stockton PS, Trempus CS, *et al*: Effects of fixation on RNA extraction and amplification from laser capture microdissected tissue. *Mol Carcinog* 25:86–91, 1999
16. Heid CA, Stevens J, Livak KJ, Williams PM: Real time quantitative PCR. *Genome Res* 6:986–994, 1996
17. Gibson UE, Heid CA, Williams PM: A novel method for real time quantitative RT-PCR. *Genome Res* 6:995–1001, 1996
18. Cohen CD, Frach K, Schlöndorff D, Kretzler M: Quantitative gene expression analysis in renal biopsies: A novel protocol for a high-throughput multicenter application *Kidney Int* 61:133–140, 2002
19. Segerer S, Cui Y, Eitner F, *et al*: Expression of chemokines and chemokine receptors during human renal transplant rejection. *Am J Kidney Dis* 37:518–531, 2001
20. Kapoor A, Morita K, Engeman TM, *et al*: Early expression of interferon-gamma inducible protein 10 and monokine induced by interferon-gamma in cardiac allografts is mediated by CD8+ T cells. *Transplantation* 69:1147–1155, 2000
21. Watarai Y, Koga S, Paolone DR, *et al*: Intraallograft chemokine RNA and protein during rejection of MHC-matched/multiple minor histocompatibility-disparate skin grafts. *J Immunol* 164:6027–6033, 2000
22. Hancock WW, Lu B, Gao W, *et al*: Requirement of the chemokine receptor CXCR3 for acute allograft rejection. *J Exp Med* 192:1515–1520, 2000
23. Grone HJ, Weber C, Weber KS, *et al*: Met-RANTES reduces vascular and tubular damage during acute renal transplant rejection: blocking monocyte arrest and recruitment. *FASEB J* 13:1371–1383, 1999
24. Pattison J, Nelson PJ, Huie P, *et al*: RANTES chemokine expression in cell-mediated transplant rejection of the kidney. *Lancet* 343:209–211, 1994